PORT SAID ENGINEERING RESEARCH JOURNAL
Faculty Of Engineering - Port Said University
Volume (21) No. (2) September 2017 pp. 231:240

Analysis of Reinforced Concrete Deep Beams Using Nonlinear Strain Model

Aya G. Abdel-Nasser [1], Tarek A. Sharaf [2], Hassan M. Ibrahim[3], and Emad Y. Abdel-Galil 4

ABSTRACT

A nonlinear strain compatibility model is considered to investigate the behavior of reinforced concrete deep beams. It is based on satisfying equilibrium of stresses and compatibility of strains at all layers of the beam cross-section. A VISUAL BASIC code is developed for this model. Strain distribution over the cross section depth in deep beams is different from shallow beams, and varies according to the case of loading, the span-to-depth ratio (*L/h*), and the structural system. The experimental values of strain over the cross-section depth for different cases for simply supported deep beams, are extracted from the available literature. Based on these values, simplified equations for strain profiles for each case is proposed to use them in the present model. A key feature of the model is the ability to illustrate the effect of shear deformation of the cross section. The model is validated by comparing predicted results with experimental ones from literature in terms of load-displacement.

Keywords: Deep beam, span-to-depth ratio (*L/h*), simplified strain profiles.

1. INTRODUCTION

Deep beams are desired in huge construction such as gravity concrete foundation, bridges, and multipurpose high-rise buildings [1]. These have many purposive applications in building structures such as transfer girders, wall footings, foundation pile caps, water tanks, bins, folded plate roof structures, floor diaphragms, brackets or corbels, and shear walls. Deep beams are defined as a load transferring structural elements which transfer a huge amount of load by compression struts to the supports with little flexure. They are characterized as being relatively short, deep, and their thickness is small relative to their span and depth. They are two dimensional members in a state of plane stress in which shear is an effective feature [2]. The behavior of deep beam is different from that of common flexural members; the strength of deep beams is basically controlled by shear rather than flexure when sufficient amounts of tension reinforcing steel are considered [3]. The stress and strain distribution along the deep beam depth are different from that in RC shallow beams.

There is much experimental and theoretical work in literature to measure the values of strain over the deep beams cross section for various span-to-depth ratios. in 1932, Dischinger used trigonometric series to estimate the stresses in continuous deep beam. Then, the Portland Cement Association (PCA) prepared an expanded version of Dischinger's paper and added solution for simply supported deep beams [4]. Chow *et al.* (1951) studied five cases of loading, and three different span-to-depth ratios were examined by using the finite difference method to solve differential equation for the stress function to solve simply supported deep beam problems. Distributions and magnitudes of flexure and shear stresses were presented in a form suitable for direct use in design [5]. Saad and Hendry (1961) presented the results of a series of photoelastic tests and showed on a number of sections a stress distribution comparison between the theoretical and experimental ones. Tests were carried out on three simply supported beams its ratios of depth *h* to span *L* were 0.67:1, 1:1, and 1.59:1 subjected to single concentrated load [6]. Mufti (1965) tested number of deep beams of different materials. Square RC deep beam under one-point loading was experimentally studied, stress distribution over the beam depth was measured also [7]. Mohammad *et al.* (2011) conducted an experimental work to investigate the behavior, design, and analysis of high strength self-compacted concrete reinforced deep beams. These beams were subjected to two

[1]*Civil Engineering Department, Faculty of Engineering, Port Said University, Port Said, Egypt, E-mail: aya.gamal20131@gmail.com*

[2]*Civil Engineering Department, Faculty of Engineering, Port Said University, Port Said, Egypt, E-mail: tarek.sharaf@eng.psu.edu.eg*

[3]*Civil Engineering Department, Faculty of Engineering, Port Said University, Port Said, Egypt, E-mail: hi_hgh@yahoo.com*

[4]*Civil Engineering Department, Faculty of Engineering, Port Said University, Port Said, Egypt, E-mail: emad0057@eng.psu.edu.eg*

–point symmetric top loading with special attention to strain distribution and neutral axis depth variation [4]. Niranjan *et al.* (2012) conducted Experimental research to determine the strength of deep beam designed by using strut –and –tie method and performed a parametric study to get strain distribution in case of deep beam also [8].

Previous researches confirmed that The behavior of reinforced concrete deep beams is more complex and differ from that of RC ordinary beams in many items. In deep beams, the transverse sections which are plane before bending do not remain plane after bending [9]. The neutral axis does not typically lie at mid-height of the deep beam cross section depth and moves away from the loading surface as the span to depth ratio (*L/h*) decreases [9]. Also, flexural stresses and strains are not linearly distributed over the deep beam depth [9]. Recently, researches on deep beams using finite element method are most common to find a description of reinforced concrete deep beams behavior of various span-to-depth ratios. Niranjan *et al.* (2012) analyzed reinforced concrete simply supported deep beams subjected to two point loads using finite element method. The behavior of deep beam was studied by considering flexural stress, flexural strain, and shear stress variations at different sections for various span to depth ratios and compared the results with Euler-Bernoulli Theory [2]. Kore and Patil (2013) used non-linear finite element method to do analysis and design of beams subjected to two points loading with three different *L/h* ratios [10]. Kusanale *et al.* (2014) analyzed and designed R.C simply supported deep beam subjected to two-point loading, with varying *L/h* ratio by using software Hypermesh11-Radioss ® [9]. Demir *et al.* (2016) performed nonlinear finite element analysis to represent the behavior of reinforced concrete deep beams subjected to one-point loading by using a commercial FE program ABAQUS ® [11] . In previous researches on deep beams using finite element method in literature, deep beams were considered to be plane stress problems.

In 2010, Sharaf proposed an analytical model for sandwich panels composed of a polyurethane foam core and glass fibre-reinforced polymer (GFRP) skins. The model based on equilibrium and strain compatibility, accounting for the core excessive shear [12]. In this study, Sharaf 's model is developed to be suitable for reinforced concrete deep beam. Beam is modeled in this study like a bar element with satisfying equilibrium of stresses and compatibility of strains at all layers of the beam cross-section using non-linear strain distribution model. In this model, shear deformations of the cross section are considered also.

2. MATERIAL MODELING

2.1. Concrete in compression

For unconfined concrete, the model of Hognestad (1951) is considered. The model assumes ascending and descending branch as a second-order parabola and an oblique straight line, respectively as shown in Figure1a [13].

For confined concrete, Scott *et al.* (1982) model is considered. The ascending branch of the model is represented by the same second degree parabola but the maximum stress for concrete is assumed to be $Kf_c^{`}$. The strain corresponding to maximum concrete stress is $2(f_c^{`}/E_c)K$, where $f_c^{`}$ is the uniaxial concrete cylinder compressive strength, E_c is The initial modulus of elasticity for concrete, and K is a factor greater than 1.00. Confinement affected the slope of the post-peak branch and empirical equations were used to present this as shown in Figure1a [14].

2.2. Concrete in tension

A linear model for tensile strain is considered as shown in Figure1b. Where f_t is the concrete tensile strength and ε_{cr} is the strain corresponding to tensile strength [15].

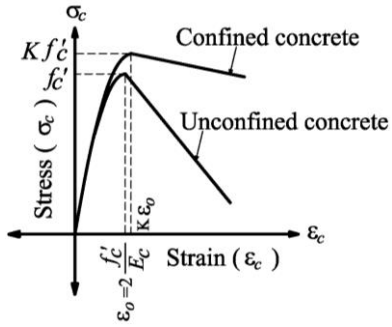

(a) Model of concrete in compression [13,14]

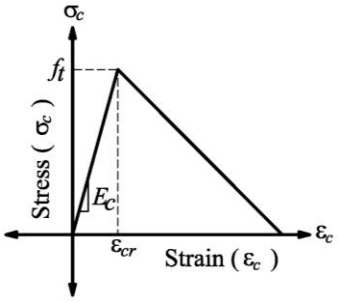

(b) Model of concrete in tension [15]

Figure 1: Stress-strain model in compression and in tension, considered in this research

2.3. Reinforcing steel

An elastic-perfectly plastic model is considered with a slight slope as shown in Figure 2. Where, E_s is The initial modulus of elasticity for steel, E_P is The modulus of

elasticity for steel after yield point, f_y is yield stress, ε_y is the strain corresponding to yield stress, and ε_u is the ultimate strain in steel at failure.

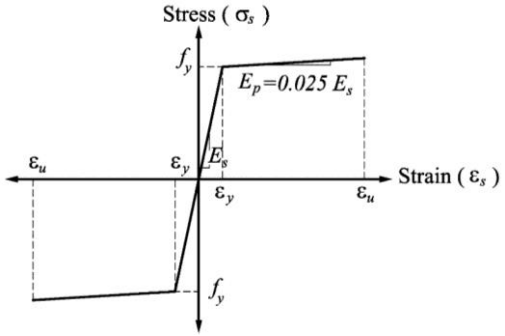

Figure 2: Theoretical stress–strain model of reinforcement used in this study [16]

3. REINFORCED CONCRETE SECTION

3.1. Strain Profile

The shape of strain profile over the cross section of deep beams is different according to the case of loading, the span-to-depth ratio (*L/h*), and the structural system. The experimental values of stress over the cross-section depth at mid-span for different cases of loading and different span-to-depth ratio for simply supported deep beams are extracted from the available literature. These values are used to propose simplified equations for strain profile for each case to study the effect of changing the shape of strain distribution on estimating the response of the deep beams in the present model.

For beams under one-point loading, with span-to-depth ratio ≥ 4.00, strain distribution, as shown in Figure 3, is assumed to be linear as follows:

$$\varepsilon_i = -\frac{\varepsilon_{max}}{y_{bar}}\, y_i \qquad (1)$$

Where;

ε_i Strain value at a specific layer over the cross section of the beam at the height y from neutral axis.

ε_{max} Compression strain value at the top surface of the cross section.

y_{bar} The distance from the neutral axis to the top surface of the cross section.

y_i The distance from the neutral axis to a specific layer; it has positive sign in compression side (top side), and negative sign in tension side (bottom side).

Based on the stress distributions shown in Figure 3 [17], it is proposed the following simpilified equations (2, 3) for strain distribution for deep beams subjected to two-points load or uniform distributed load with span-to-depth ratios equal to (2.00, 1.00) respectively, as shown in Figure 3 to use it in the present analysis.

$$\varepsilon_i = -1.75\frac{\varepsilon_{max}}{y_{bar}}\, y_i + 0.75\frac{\varepsilon_{max}}{y_{bar}^2}\, y_i^2 \qquad (2)$$

$$\varepsilon_i = -4.247\frac{\varepsilon_{max}}{y_{bar}}\, y_i + 9.462\frac{\varepsilon_{max}}{y_{bar}^2}\, y_i^2 + 10.482\frac{\varepsilon_{max}}{y_{bar}^3}\, y_i^3 + 4.267\frac{\varepsilon_{max}}{y_{bar}^4}\, y_i^4 \qquad (3)$$

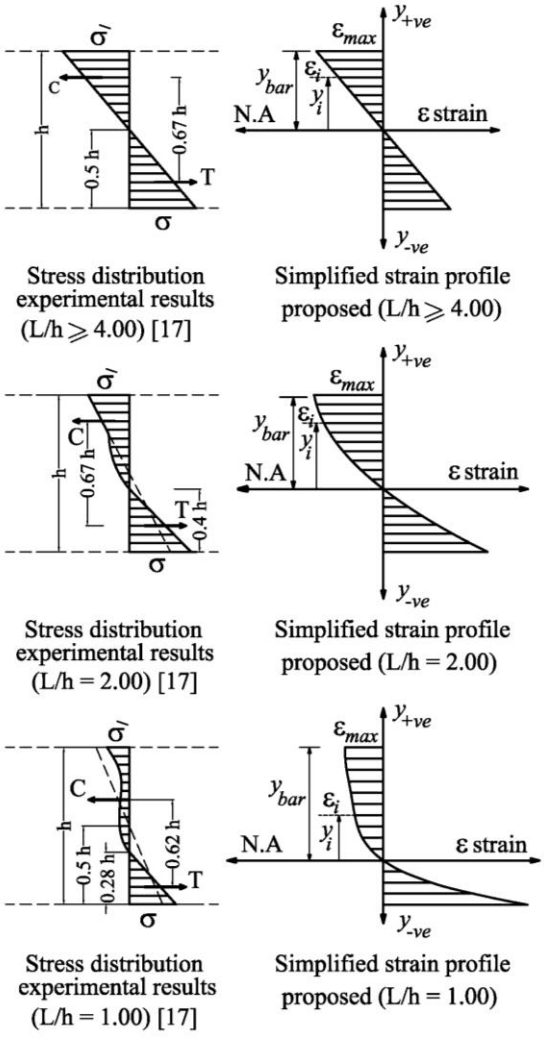

Figure 3: Experimental stress distribution results [17], vs. simplified strain profiles for deep beams under two-point or uniform loading

A simpilified strain profile shown in Figure 4, based on Mufti (1965), is proposed for deep beams with span-to-depth ratio equals to 1.00 subjected to one-point loading. Eq. 4 presents this strain distribution as follows:

$$\varepsilon_i = -0.122\frac{\varepsilon_{max}}{y_{bar}}\,y_i - 0.371\frac{\varepsilon_{max}}{y_{bar}^2}\,y_i^2 - 0.507\frac{\varepsilon_{max}}{y_{bar}^3}\,y_i^3 \quad (4)$$

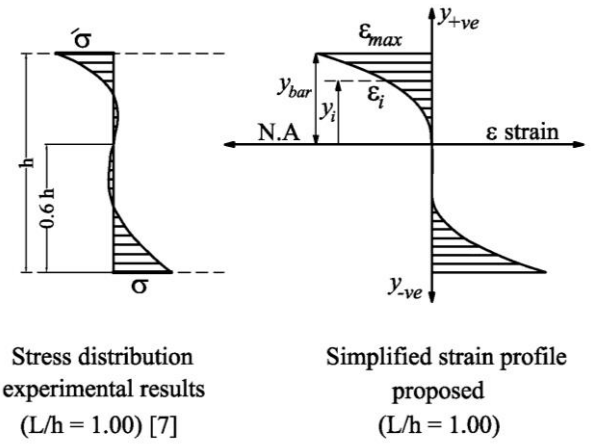

Stress distribution experimental results (L/h = 1.00) [7]

Simplified strain profile proposed (L/h = 1.00)

Figure 4: Experimental stress distribution results [7], vs. simplified strain profile for deep beams under one-point loading (*L/h*)=1.00

In deep beams with span-to-depth ratio value between the values mentioned in experimental works, it is proposed to establish a proportional equation for strain profile.

3.2. Meshing of Deep Beams

A layer-by-layer approach is adopted to integrate stresses over the cross-sectional areas of RC deep beam. The cross-section is divided into number of layers of concrete and steel (horizontal steel) according to their location. The model assumes a plane stress problem where a constant strain occurs in the cross section width direction. The span length also divided into numbers of segments according to existing vertical steel bars (stirrups) and its diameter, as shown in Figure 5.

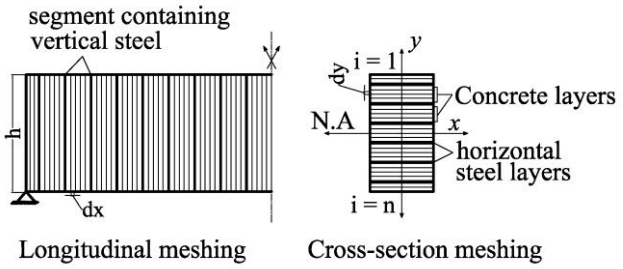

Longitudinal meshing

Cross-section meshing

Figure 5: Meshing of Deep beam

3.3. Force Equilibrium and Moments

Every cross-section of the deep beam undergoes a specific strain distribution induced in the deep beam at a given load level. Only two independent parameters are needed to establish a complete strain profile. Namely, the strain at any level, say at the extreme top face ε_{max} and the neutral axis location. From these two parameters ε_{max}, y_{bar}, the strain ε_i at any layer *i*, located at a distance y_i from the N.A, can then be determined. The normal stress in any element, either concrete or steel, σ_i is then calculated from the corresponding normal stress-strain curve, whether in tension or compression. The total cross-section force at a given stage of loading can be obtained by numerical integration of stresses over the cross section, for both concrete and steel elements. The resultant force must equal to zero in flexure to satisfy equilibrium and The corresponding moment *M* is calculated. Then the curvature $\psi = (\varepsilon_{ten}/h - y_{bar})$ is calculated and then moment-curvature response for deep beam cross section is constructed. Where ε_{ten} is the tensile strain at the bottom surface of the deep beam cross section and *h* is the beam depth.

3.4. Generation of Full Load-Deflection Response

The load-deflection response of the deep beam consists of two components, a flexural component and a shear component. In reinforced concrete shallow beams, deflections are dominated by the flexural contribution and the deflection due to shear is usually small and typically neglected. However, in deep beams, the shear displacement contribution to the overall displacement is significant and cannot be neglected.

3.4.1. Flexural Effect

Once the moment-curvature of the cross-section is obtained, the load-deflection response of the deep beam due to flexure only can be estimated for a given loading scheme. The deflection (δ_m) at any point along the span is calculated by integrating the curvatures (ψ) along the span using double integration method [12]:

$$\psi = \frac{d^2}{dx^2}\delta_m \quad (5)$$

$$\delta_m = \iint \psi(x)dxdx \quad (6)$$

Where, *dx* is the length of each segment *l* along the span as shown in Figure 5.

3.4.2.Shear Effect

The second component of the load-deflection curve is the deflection due to shear deformation as a result of the low span to depth ratio in deep beams. The deflection of any segment *l* along the span, and at a layer *i* along the depth, due to shear stress, $\delta_{v,l,i}$, in the interval *dx* along the span is equal to:

$$\delta_{v,l,i} = \gamma_{l,i}\, dx \tag{7}$$

Where the shear strain $\gamma_{l,i}$ can be calculated from the shear stress $\tau_{l,i}$ at a specific layer *i* at a given segment *l* under a specific loading condition [12].

The shear stress $\tau_{l,i}$ at any layer *i* at any segment *l* along the span can be calculated as follows:

$$\tau_{l,i} = \frac{V_l\, Q_{t,l,i}}{I_{t,l}\; b_{t,l,i}} \tag{8}$$

Where V_l is the applied shear force at segment *l* of the deep beam. $Q_{t,l,i}$ is the first moment of area for the transformed cross-section at specific layer *i*, at which shear deflection needs to be calculated about the neutral axis of the transformed section. $I_{t,l}$ is the moment of inertia for the transformed cross-section and $b_{t,l,i}$ is the width of the transformed cross section at that layer *i*.

The transformed section is established by transforming the width $b_{l,i}$ of each concrete or steel layer *i* at any segment *l* to a unified concrete material. this based on the initial material stiffness of the concrete in compression, using the following equation [12]:

$$b_{t,l,i} = b_{l,i}\left(\frac{E_{l,i}}{E_c}\right) \tag{9}$$

Where $b_{l,i}$ is the original cross-section width at segment *l* for layer *i* and $b_{t,l,i}$ is the transformed cross-section width at segment *l* for layer *i*. $E_{l,i}$ is the secant modulus of elasticity of the normal stress-strain curve of the concrete or the steel, in tension or compression, at segment *l* depending on the location of layer *i* relative to neutral axis. $E_{l,i}$ is established from the material curve of the concrete or the steel at the specific normal strain $\varepsilon_{l,i}$ of layer *i* at segment *l* at this particular loading level. E_c is the reference modulus which is the initial modulus of the concrete in compression. After calculating the shear stress, the corresponding shear strain $\gamma_{l,i}$ can be calculated as follows:

$$\gamma_{l,i} = \frac{\tau_{l,t}}{G_{l,t}} \tag{10}$$

Where $G_{l,t}$ is the shear modulus of the concrete or the steel, at segment *l* depending on the location of layer *i* relative to neutral axis, calculated as follows [15]:

$$G_{l,t} = \frac{E_{l,i}}{2(1+\upsilon)} \tag{11}$$

, Where υ is the Poisson ratio for concrete or steel.

At layer which $E_{l,i} < 0.1\ E_c$, concrete layers are neglected in shear deformation calculation.

Shear strain used to compute the shear deflection of that specific layer *i*. To calculate the total shear deflection of layer *i* at mid-span of the deep beam (span/2), the shear deflection for each segment should be summed in the longitudinal direction of the deep beam.

$$\delta_{v,i} = \sum_{l=1}^{m} \gamma_{l,i}\; dx = \sum_{l=1}^{m} \delta_{v,l,i} \tag{12}$$

Where $\delta_{v,i}$ is the total shear deflection of layer *i* specifically at mid-span, and *m* is the total number of segment along the half span [12].

As such, at any layer *i*, the shear deflection values will be different from one layer to the other, which is obviously impossible because each layer is joined to the adjacent layers and the whole cross-section must be continuous, without any gaps or overlaps. As a result, The top deflection due to shear forces at any segment, $\delta_{v,l,top}$ can be assumed as the average deflection of all layers above the neutral axis. The bottom deflection at the same segment, $\delta_{v,l,bot}$, is the average deflection of all layers below the neutral axis, as follows:

$$\delta_{v,l,top} = \frac{\sum_{i=1}^{n_{top}} \delta_{v,l,i}}{n_{top}} \tag{13}$$

$$\delta_{v,l,bot} = \frac{\sum_{i=1}^{n_{bot}} \delta_{v,l,i}}{n_{bot}} \tag{14}$$

Where n_{top} is the number of layers above the neutral axis and n_{bot} is the number of layers below the neutral axis. The total shear deflections at the deep beam mid-span at top and bottom, respectively:

$$\delta_{v,top} = \sum_{l=1}^{m} \delta_{v,l,top} \tag{15}$$

$$\delta_{v,bot} = \sum_{l=1}^{m} \delta_{v,l,bot} \quad (16)$$

$$\delta_{v,av} = \frac{\delta_{v,top} + \delta_{v,bot}}{2} \quad (17)$$

Where $\delta_{v,tob}$, $\delta_{v,bot}$, and $\delta_{v,av}$ are the total top, bottom, and average deflections due to shear, at the beam mid-span, respectively.

The final deflection δ_t will be the sum of two previous deflections, namely due to flexure and shear, as follows:

$$\delta_t = \delta_{m,l} + \delta_{v,l,av} \quad (18)$$

Where $\delta_{m,l}$ and $\delta_{v,l,av}$ are deflections at segment *l* due to flexure and shear from the average of all layers in the section respectively.

4. VALIDATION OF THE MODELS

Foster (1996) tested simply supported deep beams of different span-to-depth ratios and reinforcement arrangement under one-point loading [18]. Beam (B3.0B-5), Beam (B2.0B-5) and Beam (B1.2-3) are selected to do comparisons between the experimental results and the results obtained from the program developed for this study in terms of load vs. mid-span deflection curves. Their geometry and dimensions shown in Figure 6. Details of the beams are shown in Tables (1,2 and 3) as mentioned in experimental work [18].

Table 1: Geometry and Reinforcement of beams [18]

Beam	Dimensions in mm		Span-to-depth ratio	Web Reinforcement	
	L	***h***	***L/h***	**V**	**H**
(B3.0B-5) [18]	2350	700	3.36	-	-
(B2.0B-5) [18]	1650	700	2.36	-	-
(B1.2-3) [18]	1700	1200	1.42	8x 2w6	5x 2w6

Table 2: Concrete properties in (MPa) [18]

Beam	Compressive strength, $f_c^{`}$	Tensile strength, f_t	Modulus of elasticity, E_C
(B3.0B-5) [18]	89	6.3	50.7
(B2.0B-5) [18]	89	6.3	50.2
(B1.2-3) [18]	80	6.3	53.5

Table 3: Reinforcing steel properties in (MPa) [18]

Reinforcement bar	Yeild Stress, f_y	Modulus of elasticity, E_s
Y_{20}	440	201000
Y_{12}	440	195000
W_6	590	193000

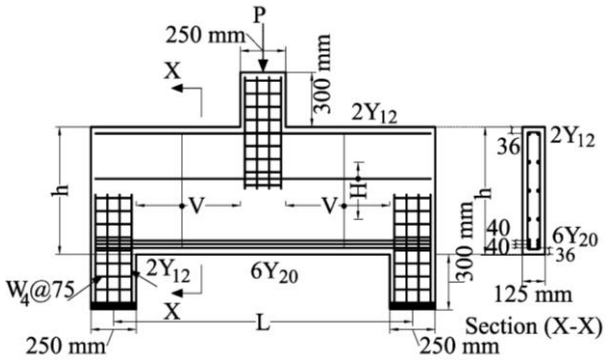

Figure 6: Geometry and dimensions of the beams [18]

According to span-to-depth ratio (*L/h*), strain distribution is chosen. For deep beam (B3.0B-5), because its span-to-depth ratio equals to 3.36, Strain distribution is assumed to be linear. For deep beams (B2.0B-5), (B1.2-3), because its span-to-depth ratios are (2.36 and 1.42 respectively) between 1.00 (equation (4)) and 4.00 (equation (1)), Strain distribution is estimated in each beam by interpolation (equations (19, 20)) as shown in Figure 7:

For beam (B2.0B-5)

$$\varepsilon_i = -0.512\frac{\varepsilon_{max}}{y_{bar}}\, y_i - 0.185\frac{\varepsilon_{max}}{y_{bar}^2}\, y_i^2 - 0.303\frac{\varepsilon_{max}}{y_{bar}^3}\, y_i^3 \quad (19)$$

For beam (B1.2-3)

$$\varepsilon_i = -0.139\frac{\varepsilon_{max}}{y_{bar}}\, y_i - 0.319\frac{\varepsilon_{max}}{y_{bar}^2}\, y_i^2 \quad (20)$$

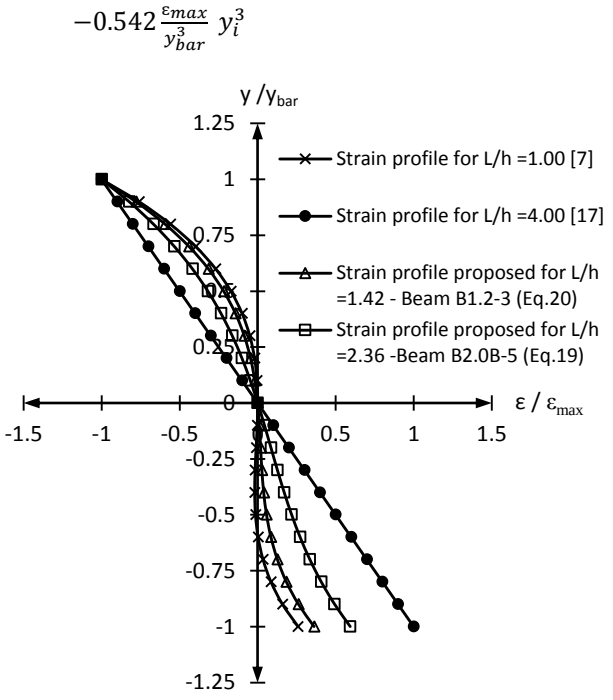

Figure 7: Strain profiles proposed in the analysis for beams B1.2-3 and B2.0B-5 tested by Foster

Islam (2012) tested simply supported deep under four-point bending. It is selected to do comparison between the results of the analytical model and the test results. Their geometry and dimensions are shown in Figure 8. The cylinder's strength was found to vary between 53 MPa to 55 MPa, the yield strength of deformed steel bars was 500 MPa [19]. According to span-to-depth ratio (*L/h*), strain distribution is chosen. Because this deep beam has span-to-depth ratio equals to 4.00, Strain distribution is assumed to be linear (Eq.1).

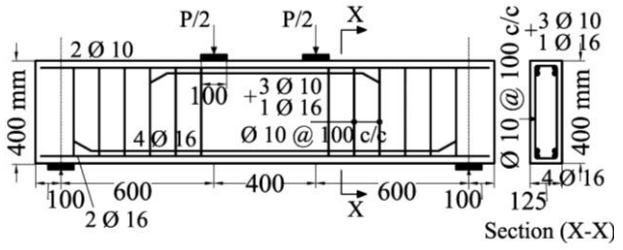

Figure 8: Geometry and dimensions of the beam [19]

Beam (B3-0.5) is selected from deep beams tested by Gedik (2011) to do comparison with the results of the analytical model. Dimensions and details of the specimen are shown in Figure 9. The compressive strength for concrete is 32.6 MPa. The yield strength of deformed steel bars used as main tensile reinforcement was 372.2 MPa [20].

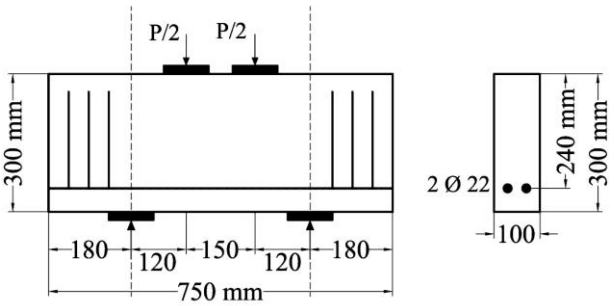

Figure 9: Geometry and dimensions of the beam [20]

Because of its span-to-depth ratio between 1.00 and 2.00, the strain profile is estimated in the following Eq. 21 by interpolation to represent strain distribution over the beam depth in this case (*L/h* = 1.3) as shown in Figure 10.

$$\varepsilon_i = -2.642\frac{\varepsilon_{max}}{y_{bar}}\ y_i + 4.768\frac{\varepsilon_{max}}{y_{bar}^2}\ y_i^2 - 5.806\frac{\varepsilon_{max}}{y_{bar}^3}\ y_i^3 + 2.68\frac{\varepsilon_{max}}{y_{bar}^4}\ y_i^4 \quad (21)$$

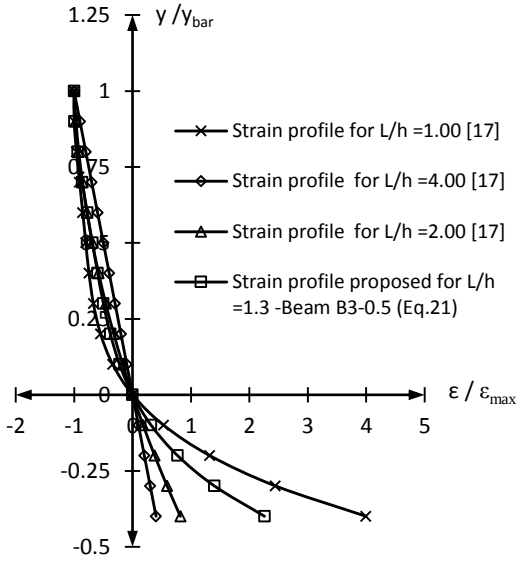

Figure 10: Strain profile proposed in the analysis for beam B3-0.5 tested by Gedik

4.1. Load deflection Response

Figures (11, 12, 13, 14 and 15) show verification results of the analytical model for the deep beams mentioned earlier for validating the model with test results in terms of load vs. mid-span deflection curves. Good agreement is achieved between the analytical model proposed in this study and the experimental test results. Figures (12a, 13a and 15a) present the effect of changing strain profile on load-midspan deflection response, while Figures (11, 12b, 13b, 14 and

15b) show the effect of shear deformation on total midspan deflection estimated by using proposed strain profile in the present model. The ratios of the model to experimental failure load are 1.06, 1.09, 1.00, 1.04 and 1.24 respectively. From these results, it can be concluded that the model developed gives reasonably accurate estimations for the displacement especially at lower loads before cracking load. At higher loads, the model shows higher stiffness until failure. This may have been caused by the approximate geometric idealization of the beam used in the program. The higher stiffness in numerical models may stem from micro-cracks reducing the stiffness of the RC member. It is known that they are present in the experimental concrete works, while numerical models do not include them. Moreover, some unknown factors may have reduced the stiffness of the experimental specimens. it is shown that using non-linear strain distribution for deep beams makes Load-midspan deflection curves approaching to the experimental curves.

4.2. Shear deformation effect

In the case of one-point loading deep beams, the effect of the shear deformation in total mid-span deflection is more pronounced than the cases of two-point loading deep beams.

Table 4 shows proportions of deflection due to flexure and deflection due to shear in overall deflection of the beams which were analyzed, respectively. These percentages for each beam are the average of the percentage values at all load stages. It is found that as the ratio of the span-to-depth ratio decreases, the effect of the shear deformation in total mid-span deflection increases.

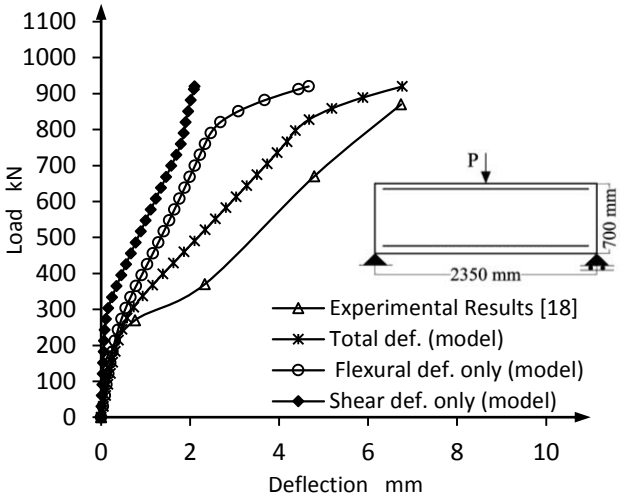

Figure 11: Load-midspan deflection response, Beam (B3.0B-5) by using linear strain profile

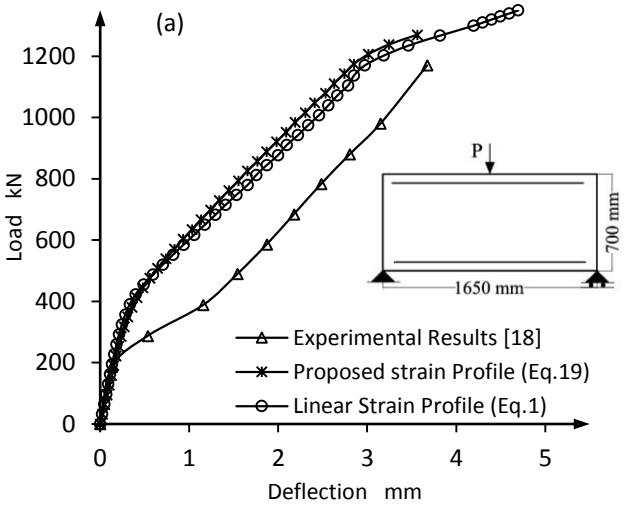

Figure 12a: Load-midspan deflection response using two different strain profiles, Beam (B2.0B-5)

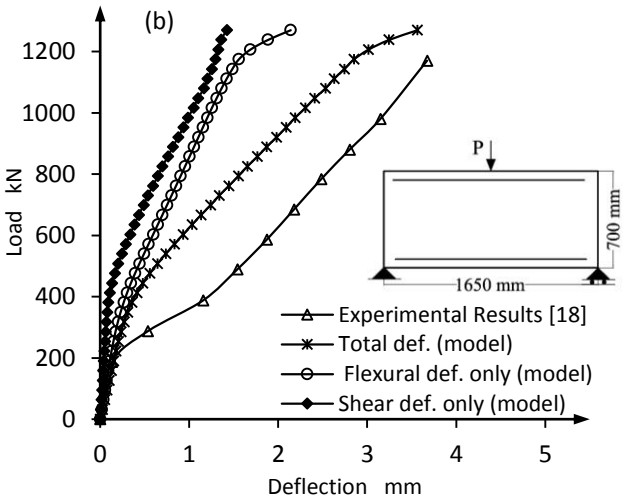

Figure 12b: Load-midspan deflection response by using proposed strain profile (Eq.19), Beam (B2.0B-5)

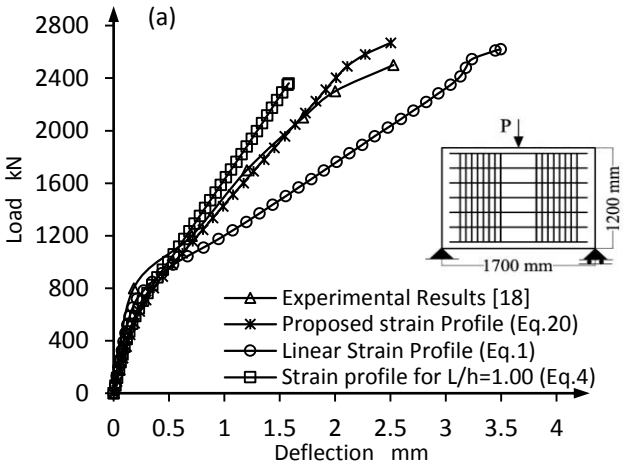

Figure 13a: Load-midspan deflection response using three different strain profiles, Beam (B1.2-3)

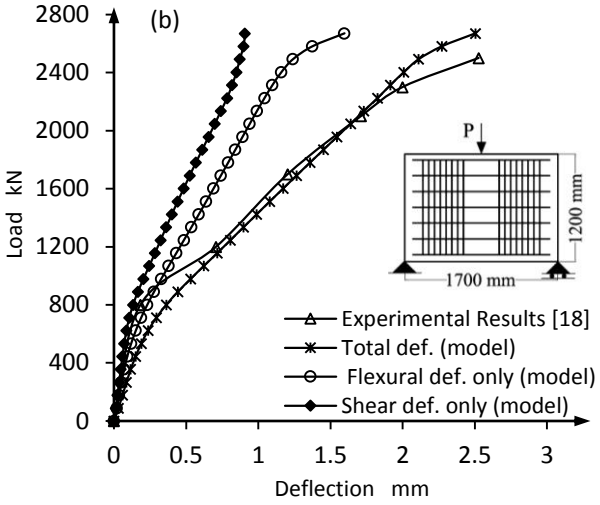

Figure 13b: Load-midspan deflection response by using proposed strain profile (Eq.20), Beam (B1.2-3)

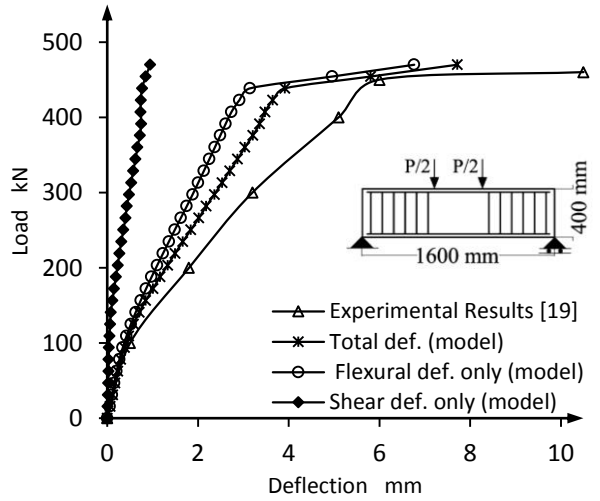

Figure 14: Load-midspan deflection response by using linear strain profile

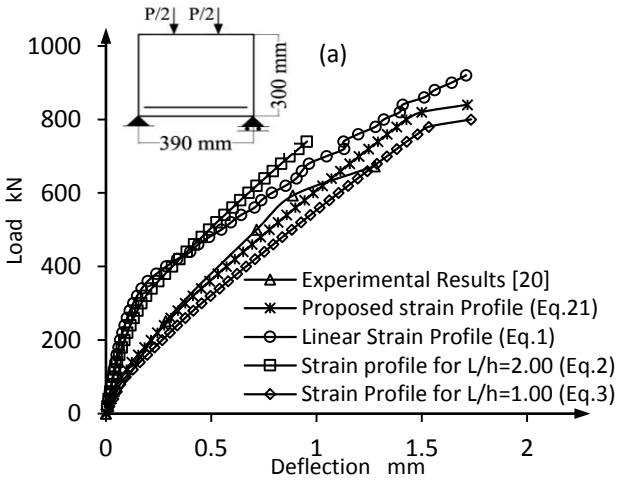

Figure 15a: Load-midspan deflection response using four different strain profiles, Beam (B3-0.5)

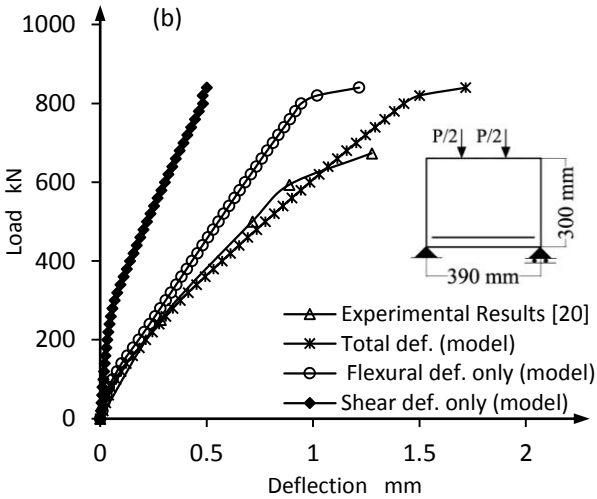

Figure 15b: Load-midspan deflection response by using proposed strain profile (Eq.21), Beam (B3-0.5)

Table 4: Percentages of deflection due to flexure and shear in overall mid-span deflection

Beam subjected to one-point loading	Span-to-depth ratio (L/h)	The percentage in overall mid-span deflection	
		Due to flexure	Due to shear
Beam (B3.0B-5)	3.36	69	31
Beam (B2.0B-5)	2.36	65	35
Beam (B1.2-3)	1.42	60	40
Beam tested by Islam	4.00	84	16
Beam (B3-0.5)	1.30	75	25

5. CONCLUSION

A nonlinear analysis is developed to predict the behavior of deep beams under point loads for different span-to-depth ratios and arrangement of reinforcement. The model proposed is simple, easy to use, and has the ability to illustrate the effect of shear deformation of the cross section. The model can isolate this shear contribution to deflection easily, and show it as a separate component. Reasonable agreement is achieved between the analytical model and the experimental test results. It is found that the strain profile for deep beams varies according to cases of loading and span-to-depth ratio. Using equations proposed in this study to represent strain distribution gives more accurate and reliable predictions of the experimental test results than linear distribution.

References

[1] T. M. Yoo, "Strength and Behaviour of High Strength Concrete Deep Beam with Web Openings," A PhD Thesis, Griffith University, Australia, 2011.

[2] B. Niranjan and S. Patil, "Analysis of RC Deep Beam by Finite Element Method," International Journal of Modern Engineering Research (IJMER), vol. 2, pp. 4664-4667, 2012.

[3] Y.J. Lafta and Kun Ye, " Specification of Deep Beams Affect the Shear Strength Capacity," Civil and Environmental Research, vol. 8, pp. 56-68, 2016.

[4] M. Mohammad, M. Z. B. Jumaat, M. Chemrouk, A. Ghasemi, S. Hakim, and R. Najmeh, "An experimental investigation of the stress-strain distribution in high strength concrete deep beams," Procedia Engineering, vol. 14, pp. 2141-2150, 2011.

[5] L. Chow, H .D. Conway, and G. Winter, "Stresses in deep beams," A.S.C.E., vol. 118, pp. 686-708, 1953.

[6] S. Saad and A. Hendry, "Gravitational stresses in deep beams," Structural Engineer, vol. 39, pp. 185-8, 1961.

[7] A. A. Mufti, "Stresses in deep beams," A master Thesis, McGill University, Montreal,1965.

[8] B. Niranjan and S. Patil, "Analysis and Design of deep beam by using Strut and Tie Method," IOSR Journal of Mechanical and Civil Engineering IOSR-JMCE, vol. 3, pp. 14-21, 2012.

[9] A. A. Kusanale, S. B. Kadam, and S. N. Tande, " Analysis and Design of R.C. Deep Beam by Finite Element Method," International Journal of Emerging Engineering Research and Technology, vol. 2, pp. 166-169, 2014.

[10] S. D. Kore and S. Patil, "Analysis and Design of RC Deep Beams Using Code Provisions of Different Countries and Their Comparison," International Journal of Engineering and Advanced Technology, vol. 2, pp. 166-169, 2013.

[11] A. Demir, H. Ozturk, and G. Dok, "3D Numerical Modeling of RC Deep Beam Behavior by Nonlinear Finite Element Analysis," Disaster Science and Engineering, vol. 2, pp. 13-18, 2016.

[12] T. A. Sharaf, "Flexural Behaviour of Sandwich Panels Composed of Polyurethane Core and GFRP Skins and Ribs," A PhD Thesis, Queen's University, Canada, 2010.

[13] E. Hognestad, "A Study of Combined Bending and Axial Load in Reinforced Concrete Members," University of Illinois Engineering Experiment Station, Bulletin Series No. 399, Bulletin No. 1, 1951.

[14] M. K. M. Reddiar, "Stress-strain model of unconfined and confined concrete and stress-block parameters," A master Thesis, Texas A&M University, USA, 2009.

[15] W. F. Chen, "Plasticity In Reinforced Concrete," McGraw-Hill Book Company, United States of America, 1982.

[16] X. Gu, X. Jin, and Y. Zhou , "Basic Principles of Concrete Structures, " Springer-Verlag Berlin Heidelberg and Tongji University Press, 2016.

[17] A. Fuentes, "Reinforced Concrete After C racking, second edition," Oxford& IBH publishing CO. PVT. LTD., New Delhi by arrangement with Editions Eyrolles, 1995.

[18] S. J. Foster and R. I. Gilbert, "Tests on high-strength concrete deep beams," A PhD Thesis, The University of New South Wales, Sydney, Australia, 1996.

[19] S. M. S. Islam and A. Khennane, "Experimental Verification of Automated Design of Reinforced Concrete Deep Beams," SIMULIA Customer Conference, Australia, 2012.

[20] Y. H. Gedik, "Experimental and numerical study on shear failure mechanism of RC deep beams," A PhD Thesis, Nagoya University, JAPAN, 2011.